Eng. Sci., 2022, **19**, 215–224

Engineered Science

DOI: https://dx.doi.org/10.30919/es8d687

Mechanochemical Synthesis of Platinum Nanoclusters Supported Cordierite for Enhanced Catalytic Oxidation of Toluene

Peng Du,[1,2] Chaoliang Lin,[1] Ruyue Wang,[1,2] Xian He,[1] Ru Zhang,[2] Zhaofeng He,[3,*] Geng Chang,[4] Xuchao Pan,[4,*] Kai Huang[1,*] and Ming Lei[1,*]

Abstract

Developing a low cost and high efficiency synthetic pathway is essential for the large-scale application of supported noble metal catalysts in many important environmental catalytic reactions, especially for volatile organic compounds (VOCs) catalytic oxidation. In this study, we report a facile chemical wet ball-milling method to control the metal-support interactions and platinum (Pt) nanoclusters (1.12 ± 0.23 nm) supported cordierite honeycomb ceramic (CHC) catalysts with enhanced toluene oxidation performance is obtained. The optimized Pt/CHC catalyst with Pt loading as low as 1.0 wt.% could convert 90% toluene (1000 ppm) to CO_2 at about 160 °C under a space velocity of 40000 mL g^{-1} h^{-1}. The catalyst also exhibits a low apparent activation energy of 44.1 kJ mol^{-1}, high stability for more than 60 h and moisture resistance properties under reaction condition. It is concluded that the high adsorbed oxygen species concentration, better low-temperature reducibility, and synergistic effect between Pt nanoclusters and CHC support is responsible for enhanced catalytic performance. Furthermore, the present wet ball-milling synthetic strategy paves a new avenue for mass production of highly efficient supported noble metal catalysts for environmental applications.

Keywords: Catalytic oxidation; Ball-milling; Noble metal; Metal-support interaction; Absorbed oxygen.
Received: 13 March 2022; Revised: 24 March 2022; Accepted: 30 March 2022.
Article type: Research article.

1. Introduction

In recent years, increasing levels of air pollution has been universally recognized as a global environmental and social concern.[1-4] Being a major source of gaseous pollutants, volatile organic compounds (VOCs) are widely used in industrial processes including painting, pharmaceuticals, dyeing, and petrochemicals as solvent or reagent, causing severe adverse influence on human health and ecological environment, *e.g.*, photochemical smog and ozone pollution.[5-8] Among various techniques utilized to control VOCs emission, catalytic oxidation was demonstrated as an efficient and cost-effective technology due to lower energy consumption and lack of secondary pollution compared to conventional thermal methods.[9-12] Tremendous efforts have been devoted on developing catalysts with superior performance and stability, while their cost and controllable preparation methods at large scale have drawn limited attention.

Represented by cordierite honeycomb ceramics (CHC), porous ceramic materials have emerged as a promising candidate for applications in filtration and separation, catalyst substrates and pollution prevention/control.[13-15] It is also a secondary support of monolithic catalysts commonly used in practical VOCs emissions to facilitate the mass transfer and reaction processes. Though offering advantages such as resistance to high temperature, chemical corrosion and excellent porosity, there still remains concerns on homogeneity, reliability and durability of coating catalytic

[1] *State Key Laboratory of Information Photonics and Optical Communications, School of Science, Beijing University of Posts and Telecommunications, Beijing 100876, China.*
[2] *Beijing Key Laboratory of Space-ground Interconnection and Convergence, Beijing University of Posts and Telecommunications (BUPT), Xitucheng Road NO.10, Beijing, 100876, China.*
[3] *School of Artificial Intelligence, Beijing University of Posts and Telecommunications, Beijing 100876, China.*
[4] *Ministerial Key Laboratory of ZNDY, Nanjing University of Science &Technology, Nanjing 210094, China.*
**E-mail:* mlei@bupt.edu.cn (M. Lei); zhaofenghe@bupt.edu.cn (Z. F. He); pxchxc@njust.edu.cn (X. C. Pan); huang-kai@bupt.edu.cn (K. Huang)

components, hindering its further large-scale applications.[16,17] It can be determined from an abundance of researches that the irreducible oxides of elements contained in cordierite (*e.g.*, SiO_2, Al_2O_3, MgO) are also favorable substrate materials for catalysts toward environmental purification and have been widely applied in the fabrication of supported noble metal catalysts, which is considered as the most promising advanced catalyst because of unique physical and chemical properties and extremely high specific activities at low temperatures.[18-21] For example, nanoscale particles and clusters of platinum (Pt) have been proved to facilitate the complete oxidation of VOCs such as ethyl acetate and toluene, and a loading amount of up to 1.0 wt.% is optimal for the synthesis of such catalysts in a cost-effective method.[22,23] Meanwhile, despite of the structural design and performance optimization of catalysts which directly associated with energy consumption, their controllable preparation process and economic limitations are also the key-points to be considered in their scalable applications.[24-26] Recently, mechanochemical treatment containing ball-milling and related techniques has recently grown in interest for nanomaterials synthesis in fields like environmental treatment, electrocatalysis, renewable energy and industrial production.[27-29] Compared to the traditional synthesis like impregnation, calcination and co-precipitation, mechanochemical pathways can be performed to avoid local concentrations or agglomerations under mechanical forces with minimal solvent usage and fabrication cost.[30-32] Such economical preparation with controlled morphology and properties by easy scale-up procedures facilitates the practical application of heterogeneous catalysts. Furthermore, the effective reduction into desired nanostructures and immobilization on substrates of noble-metal precursors, as well precisely modulate the metal-support interactions make it a novel and feasible choice for synthesis of supported noble metal catalysts.[33,34] Therefore, it is imperative and fascinating to investigate the mechanically assisted preparation method and potential application of Pt nanostructure immobilized on cordierite honeycomb ceramics with low cost and ready availability to meet the requirements for advanced catalytic performance in VOCs oxidation.

In this study, we reported a facile chemical wet ball-milling strategy for preparation of Pt nanoclusters immobilized on cordierite substrate (Pt/CHC) as efficient catalysts for the catalytic oxidation of toluene. To understand and systematically evaluate the catalytic performance, Pt/CHC catalysts with various Pt loading amounts (0.2, 0.5 and 1.0 wt.%) under the same parameter of ball-milling treatment. The morphology, structure and catalytic activity for toluene catalytic degradation were investigated in detail by a series of characterizations, and the enhancement mechanism of Pt nanoclusters immobilization to catalytic oxidation performance was refined. The metal-support interaction as well as oxygen vacancy at the interface between Pt species and cordierite substrate were optimized by mechanochemical treatment, offering better adsorption and activation of reactants, thus leading to excellent catalytic activity and stability for toluene combustion. This work presents a promising strategy for the scalable development of high-performance supported noble metal catalysts for environmental treatment.

2. Experimental section

2.1 Materials

Cordierite honeycomb ceramic (CHC, $2MgO{\cdot}4Al_2O_3{\cdot}5SiO_2$, supplied by Hyperion Co., Ltd.), absolute ethanol (C_2H_5OH, 99.8%, Aladdin), Tetraammineplatinum dinitrate ($[Pt(NH_3)_4](NO_3)_2$, Aladdin) and deionized water were used as received without further purification except for special declaration in this work.

2.2 Synthesis of Pt nanoclusters supported CHC catalysts

In a typical synthesis, 500 mg pristine bulk CHC substrate was firstly ground into powder by a mechanical ball milling method at a speed of 300 rpm and then sonicated in a high-power sonic bath (100 W) into 30 mL of ethanol solvent for 40 min to form a homogeneous suspension. 30 mg $[Pt(NH_3)_4](NO_3)_2$ was immersed into 500 μL deionized water and sonicated to achieve a uniformly suspension as Pt precursor solution. The as-obtained suspensions of CHC substrate and Pt precursor was then continuously stirred for 2h to ensure the sufficient adsorption and reducing of Pt species. The post-reaction solution was transferred into a corundum tank and ball-milled at a speed of 150 rpm for 30 minutes. Finally, the Pt nanoclusters supported CHC catalyst with a Pt loading amount of 1.0% (denoted as 1.0% Pt/CHC) was obtained by vacuum filtration and drying the solution afterward. The Pt nanoclusters supported CHC samples with different Pt loading amounts of 0.5 wt.% and 0.2 wt.% were obtained under the same ball-milling parameters by changing the volume of Pt precursor solution added into the reaction system (denoted as 0.5% Pt/CHC and 0.2% Pt/CHC, respectively).

2.3 Characterization

The microstructure and energy dispersion spectroscopy (EDS) elemental mapping images of samples were characterized by aberration-corrected high-resolution transmission electron microscopy (HRTEM, JEOL JEM-ARM200F). The morphology of samples was also characterized by field emission scanning electron microscope (FE-SEM, LEO-1530, Zeiss, Germany). The concentration of Pt element was determined by inductively coupled plasma atomic emission spectrometry (ICP-AES) analysis performed on a Thermo ICAP-6300 instrument. The structural characterizations of phase and chemical bonds were performed by powder X-ray diffractometry (XRD, D/max 2500 V, Rigaku) using a Cu Ka as radiation source, and X-ray photoelectron spectroscopy (XPS, ESCALAB 250Xi, Thermo Fisher Scientific). To investigate the reducibility of as-prepared catalysts, the H_2-TPR characterization was carried on a Micromeritics Auto Chem II 2920 from 50 °C to 800 °C, with a heating rate of

10 °C min^{-1}. In-situ diffuse reflectance infrared Fourier transform spectroscopy (DRIFTS) for toluene oxidation is carried out on Bruker Tensor-II instrument, equipped with a mercury cadmium telluride (MCT) detector cooled by liquid nitrogen. The samples were firstly pretreated at 250 °C for 40 min in O_2 flow and then cooled to 100 °C. The spectrum is recorded and used as the background. Toluene was introduced into the sample by carrier gas. The spectra were collected under steady state with a heating rate of 5 °C min^{-1}.

2.4 Catalytic activity test

The Catalytic activities of samples were evaluated in a continuous flow fixed-bed quartz tubular microreactor (*i.e.* 6.0 mm). 50 mg of the sample sieved to a particle size of 40-60 mesh was diluted with 250 mg of quartz sands (40-60 mesh) to minimize the influence of hot spots. The N_2 stream which passes through liquid toluene in an ice-water isothermal bath is mixed with another N_2 and O_2 gas mixture with a total flow of 33.3 mL min^{1-} to obtain the toluene vapor concentration of 1000 ppm and the space velocity (SV) was 40000 mL g^{-1} h^{-1}. For water vapor introduction, 5.0 vol% H_2O was introduced by passing the feed stream through a water saturator at 34 °C. Before activity test, each sample was treated in an oxygen flow of 20 mL min^{-1} at 250 °C for 1 h. The inlet and outlet gases were analyzed online by a Shimadzu gas chromatography (GC-14C) equipped with a flame ionization detector (FID) and a thermal conductivity detector (TCD).

The catalytic oxidation activities for toluene of the samples were evaluated using the temperatures required for achieving toluene conversions of 50 and 90, respectively (T_{50} and T_{90}). Toluene conversion was defined as follows:

$$\alpha = (C_{inlet} - C_{outlet}) / C_{inlet} \times 100\% \quad (1)$$

where, the C_{inlet} and C_{outlet} represents the inlet and outlet toluene concentrations in the feed stream.

The activation energies are calculated using the Arrhenius relationship as follows:

$$\ln k = -E_a / RT + \ln A \quad (2)$$

where, E_a represents the apparent activation energy and A represents the pre-exponential factor.

Furthermore, the values of TOF_M and specific reaction rates were used to compare the catalytic activities of catalysts and the values were defined as follows:

$$TOF_M = mC_0/n_M \quad (3)$$

$$\text{specific reaction rates} = mC_0/w_M \quad (4)$$

where, m is the toluene conversion at a typical temperature (*e.g.*, 140 °C), C_0 (mol/s) is the initial toluene concentration per second, n_M (mol) is the molar amount of noble metal or oxide, and w is the weight of noble metal or oxide.

3. Results and discussion

3.1 Synthesis and morphology

In order to achieve the efficient and accurately modifications of catalytic active components on cordierite honeycomb ceramic, which has been extensively applied in the field of monolithic catalysts, we propose a mechanochemical ball milling strategy for the synthesis of Pt/CHC catalysts. As illustrated in Fig. 1a, The bulk lumps of CHC was first mechanically crushed into powder by ball milling method for homogeneously dispersion. Then, the post-milled CHC substrate was immersed into ethanol solvent and adequately sonicated to achieve a uniformly suspension. A water solution of $[Pt(NH_3)_4](NO_3)_2$ was introduced into the CHC suspension and continuously stirred for 40 min. The solution of Pt precursor and CHC substrate was further transferred into a

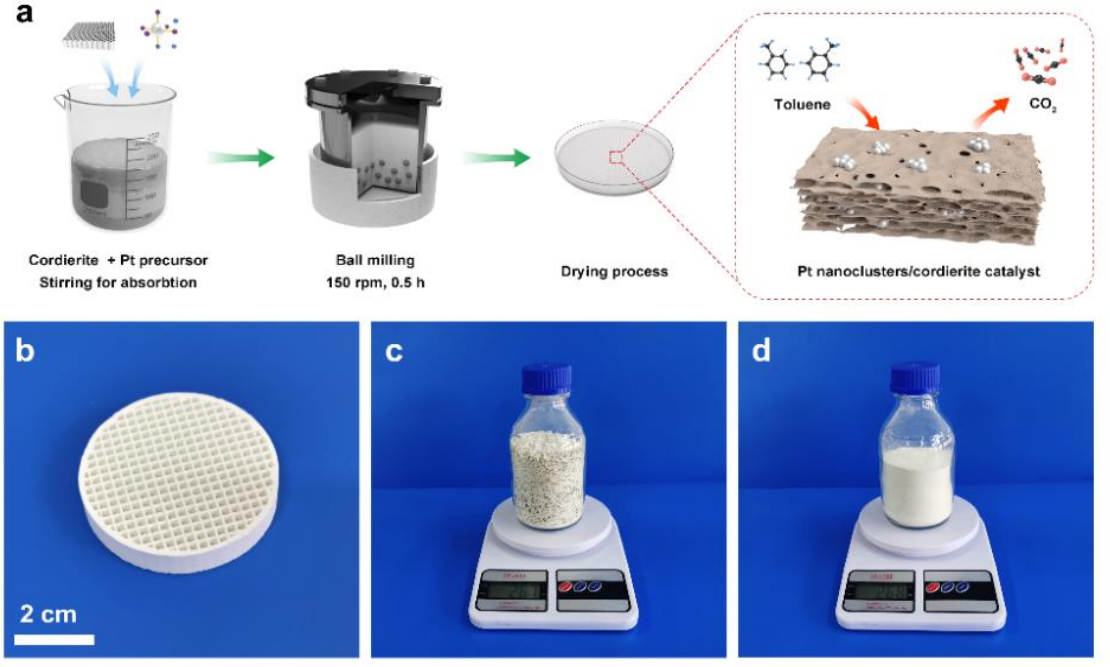

Fig. 1 (a) Synthetic process of catalysts by chemical wet ball-milling strategy. Optical photographs of (b) the CHC monolith, (c) pristine bulk CHC and (d) 1.0% Pt/CHC catalyst at large scale.

corundum tank and ball milling at room temperature. The Pt precursor was chemically reduced into relatively small-sized nanoclusters and adequately immobilized on the CHC substrate under the mechanochemical effects provided by ball-milling. Small amount of ethanol was introduced into the reaction system to act as both a weak reducing agent with slow kinetics and a solvent to improve the homogeneity of products.[35] Fig. 1b presents an optical photograph of a commercial cordierite honeycomb ceramic monolith with low cost and ready availability, which can be flexibly manufactured corresponding to required specification. The pristine bulk cordierite substrate and as-synthesized 1.0% Pt/CHC catalyst are depicted in Figs. 1c-d, demonstrating that the mechanochemical strategy facilitates the large-scale preparation of such catalysts.

The morphology and microstructure of Pt immobilized CHC catalysts were investigated by SEM and HRTEM. Compared to the SEM images of pristine CHC substrate in larger sizes in Figs. 2a-c, the Pt/CHC catalyst treated by mechanochemically ball-milling exhibited the uniformly distributed island-like structures with an average size decreased into about 500 nm (Figs. 2d-f), favoring the subsequently sufficient dispersion and homogenous loading of Pt nanostructures on surface of CHC substrate. The HRTEM images of the as-synthesized 1.0% Pt/CHC catalyst at different magnifications were displayed in Figs. 3a-c, suggesting that the small-sized Pt nanoclusters are successfully anchored on the surface of CHC substrate with an average size of 1.12 ± 0.23 nm, the size distribution histogram based on a corresponding typical TEM image of which were shown in Fig. S1. Furthermore, the homogeneous distribution of Pt nanoclusters and elements composition of the 1.0% Pt/CHC catalyst was also revealed by the energy dispersive spectroscopy (EDS) elemental mapping of O, Si, Mg, Al and Pt in Figs. 2d-i. The loading amount of Pt in the catalyst is totally as low as 0.2, 0.5 and 1.0 wt.%, which is precisely controlled with the change of Pt precursor solution volume and determined by ICP-AES (shown in Table S1). Therefore, the results of morphology characterizations corroborate the formation of the desired material by design.

3.2 Structural characterizations

XRD and XPS characterizations were further investigated to get insight into the crystal structure and chemical valence state of as-prepared catalysts. As shown in Fig. 4a, the characteristic diffraction peaks corresponding to cordierite phase (JCPDS PDF#48-1600) can be observed for pristine CHC substrate and all of the Pt immobilized catalysts with a loading amount range of 0.2~1 wt.%.[36] No obvious Pt phase can be indexed in the XRD pattern of Pt/CHC samples, demonstrating the uniformly distribution of small-sized Pt nanoclusters and no obvious changes were induced to the crystal phase of cordierite due to the modification of Pt.[37,38] To identify the chemical state of Pt, O elements and analyze the metal-support interaction in these Pt/CHC catalysts, 1.0% Pt/CHC sample is used as a substitute for XPS characterization because the low Pt signal of 0.2 and 0.5 % Pt/CHC samples cannot be well measured well due to the detect limit. All of the binding energies are calibrated by using a C 1s at 284.8 eV as internal standard. The XPS survey spectrum of both CHC and 1.0% Pt/CHC was shown in Fig. S3, verifying the presence of elemental Mg, Al, Si and O. It should be noted that the Pt 4d spectrum was used in this study because of the Al 2p spectrum overlaps with that of Pt 4f. As displayed in Fig. 4b, the Pt 4d XPS spectrum of the 1.0% Pt/CHC sample (310-322 eV) can be deconvoluted into three peaks corresponding to species typical for Pt^0 (~514.1 eV), Pt^{2+} (~316.2 eV) and Pt^{4+} (~318 eV), indicating that the dominate Pt element presents as oxidation state of Pt^{2+} and Pt^{4+}on the surface of CHC substrate.[39] O 1s XPS spectrum was performed to obtain an

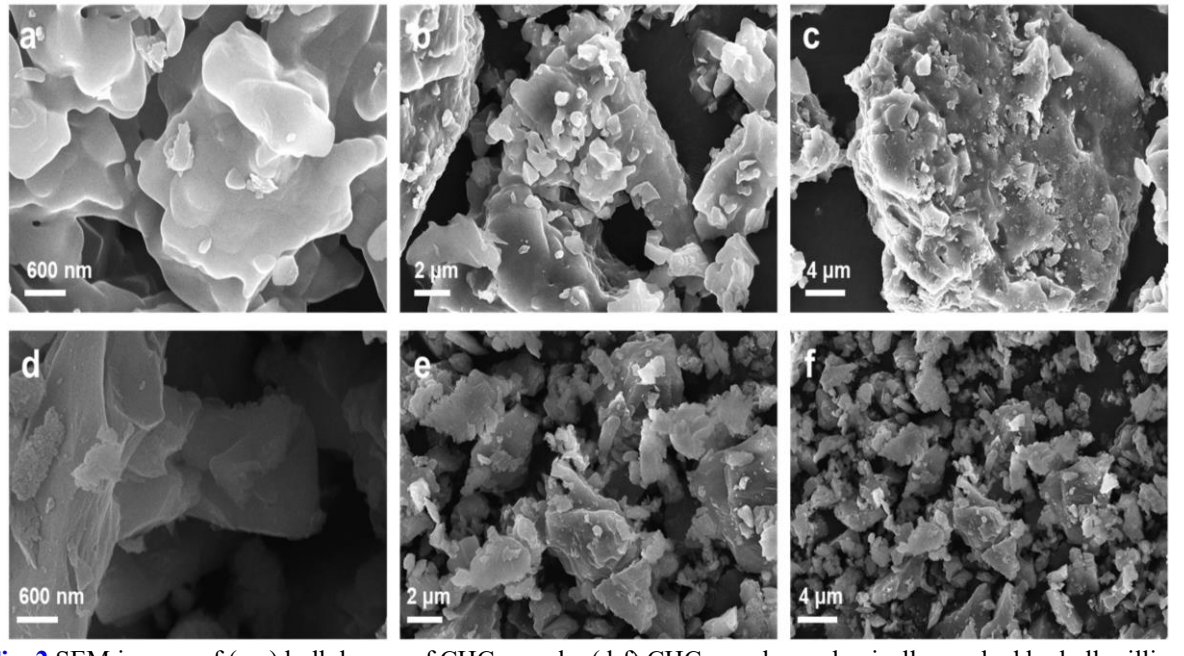

Fig. 2 SEM images of (a-c) bulk lumps of CHC sample; (d-f) CHC sample mechanically crushed by ball milling.

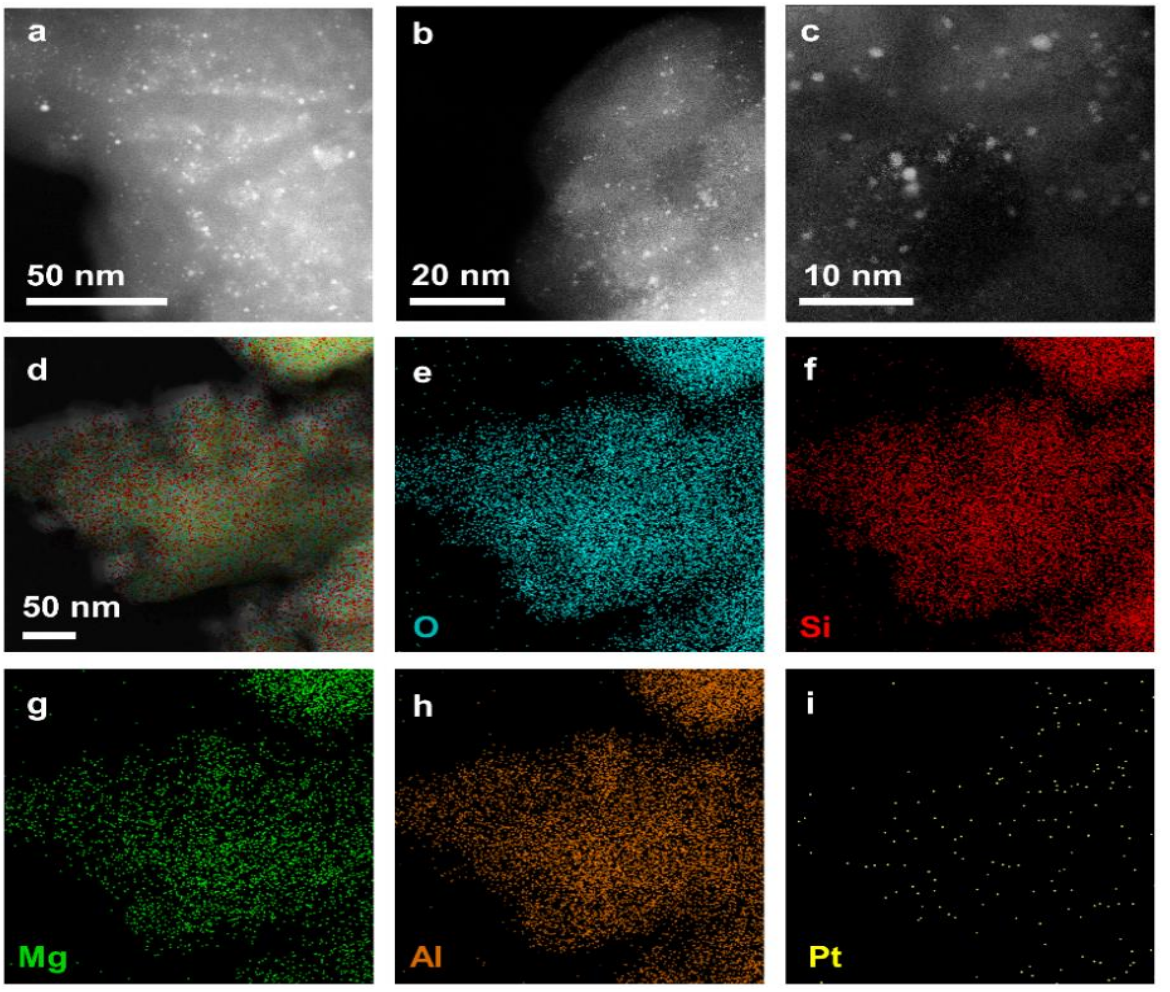

Fig. 3 (a-c) HRTEM images of the as-synthesized 1.0% Pt/CHC catalyst. (d-i) EDX elements mapping images for 1.0% Pt/CHC of O, Si, Mg, Al and Pt elements.

in-depth understanding of the migration and transformation ability of surface oxygen properties in Fig. 4c. The spectra of both samples can be fitted into two peaks at 530.6 and 531.7 eV, assigned to the lattice oxygen species (O_{latt}) and surface absorbed oxygen species (O_{abs}), respectively. The ratio of O_{abs} in the 1.0% Pt/CHC sample reflecting the content of reactive oxygen species with stronger migration ability was higher than that of CHC substrate.[40,41] It can be suggested that the immobilization of Pt nanoclusters facilitates the formation of more reactive oxygen species, further promoting the catalytic oxidation processes. H_2 TPR experiments were carried out to investigate the reducibility of the CHC substrate and Pt/CHC samples (Fig. 4d). Only one reduction peak centered at 282 °C could be observed for CHC substrate, which was attributed to the reduction of the bulk cordierite species and almost irreducible in this temperature range. With the immobilization of Pt nanoclusters, the reduction peak appeared in the range of 534-544 °C, assigned to the reduction of high-valence Pt species and the possible reduction of the surface cordierite. What's more, the reduction peak appeared at 445 °C of 1.0% Pt/CHC was due to the reduction of large amount of reducible Pt^{4+}. Compared to the temperature (282 °C) at the first reduction peak of CHC, the temperature for the reduction of samples with increasing Pt contents were shifted to a lower temperature. Above results suggested that there was presence of a strong interaction between Pt and CHC substrate, giving rise to the improvement in low-temperature reducibility of the Pt/CHC samples and beneficial influence for the catalytic activity enhancement. It can be evidenced that the total H_2 consumption (0.203 mmol/g $_{cat}$) of 1.0% Pt/CHC was much higher than those of 0.5, 0.2% Pt/CHC and CHC substrate (0.104, 0.085 and 0.0026 mmol/g $_{cat}$). The higher total H_2 consumption demonstrated more amounts of adsorbed oxygen, which was in good agreement with XPS results.[42,43] The in-situ DRIFTS spectra of the as-prepared 1.0% Pt/CHC catalyst and CHC substrate at different temperatures were carried out to detect the oxidation of toluene reactant. The bands in the range of 2880-3088 cm^{-1} were ascribed to the vibrations of C-H bands of toluene molecules, while the bands between 2300-2350 cm^{-1} could be assigned to the vibration of CO_2 production from the catalytic oxidation.[44,45] As for 1.0% Pt/CHC sample (Fig. 4e), the conversion of toluene could be observed clearly when the temperature increased, which also accompanied with an obvious increase of signals corresponded to CO_2. It can be confirmed that the oxidation of toluene to CO_2 could be proceed on the surface of 1.0% Pt/CHC catalyst at lower

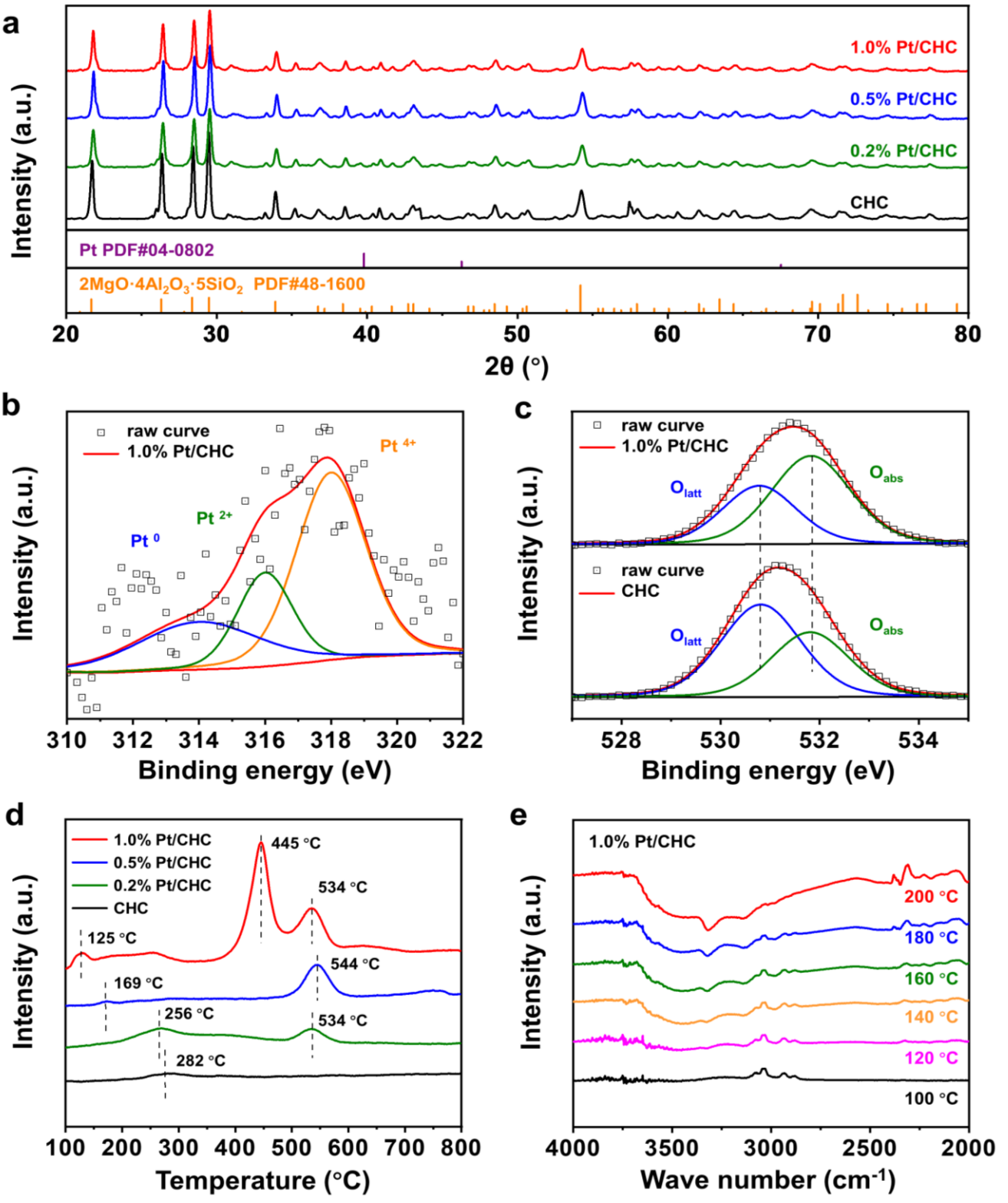

Fig. 4 (a) XRD patterns of Pt/CHC catalysts with different Pt loading amounts and CHC substrate. High-resolution XPS spectra of (b) O 1s and (C) Pt 4d for CHC and 1.0% Pt/CHC catalysts. (d) H_2-TPR profiles of Pt/CHC catalysts with different Pt loading amounts and CHC substrate. (e) In-situ DRIFTS spectra of toluene oxidation over 1.0% Pt/CHC catalyst.

temperatures. In contrast, the in-situ DRIFTS spectra of CHC substrate was presented in Fig. S2, nearly no change could be observed over the bands of toluene and few signals assigned to CO_2 were observed in the temperature range from 100 to 200 °C, showing that oxidation of toluene could hardly occur over the pristine CHC substrate.

3.3 Catalytic performance

The catalytic performance of toluene oxidation over the Pt/CHC catalysts was demonstrated by a continuous-flow

fixed-bed reactor and analyzed by GC, the schematic diagram of which was shown in Fig. 5. As presented in Fig. 6a, the pristine CHC exhibited poor activity for toluene oxidation and the toluene conversion increased with the rise of reaction temperature, suggesting that small loading amounts of Pt nanoclusters onto CHC surface could significantly enhance the catalytic performance. The high conversion rate from toluene to CO_2 production could be experimentally proved by GC images in Fig. S4 and changes of corresponding peak areas in Table S2. The temperatures required for 10%, 50% and 90% conversion of toluene (denoted as T_{10}, T_{50} and T_{90}) over 1.0% Pt/CHC catalyst were 122, 148 and 160 °C, while the T_{50} and T_{90} values for 0.5% Pt/CHC (145, 173 and 190 °C) and 0.2% Pt/CHC (165, 195 and 208 °C) were obviously higher than those of the 1.0 % Pt/CHC sample (Fig. 6b). Additionally, the apparent activation energies (E_a) are evaluated by using the Arrhenius relationship in Fig. 6c. The E_a over 1.0% Pt/CHC was 44.1 kJ mol^{-1}, followed by 0.5% (49.3 kJ mol^{-1}), 0.2%

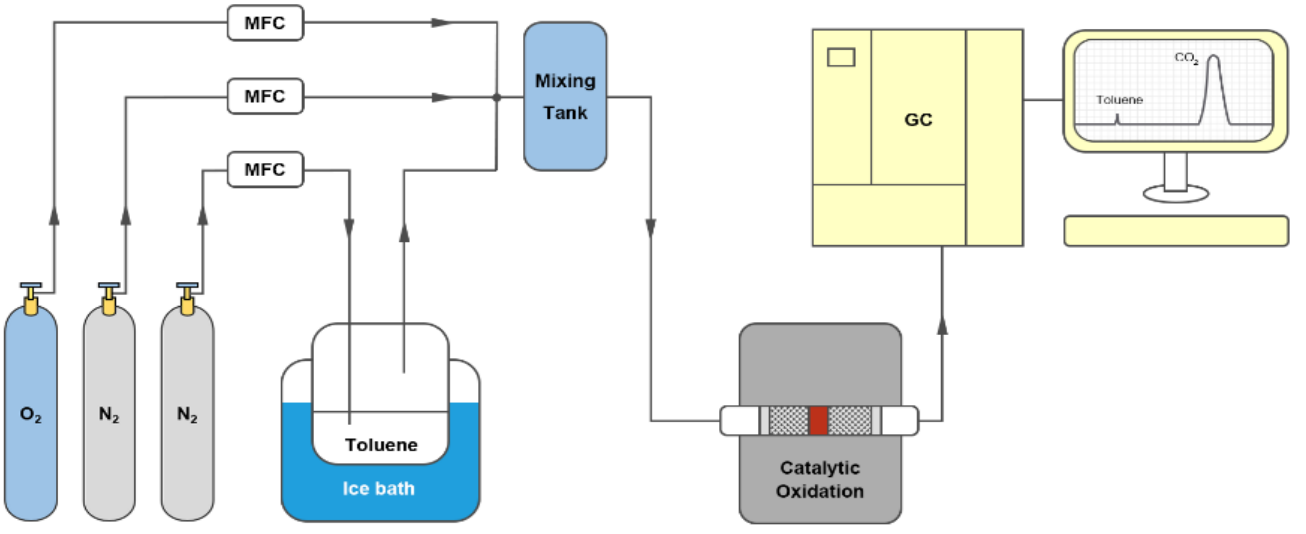

Fig. 5 Schematic diagram of the experimental setup for testing catalytic performance of synthesized catalysts for toluene oxidation.

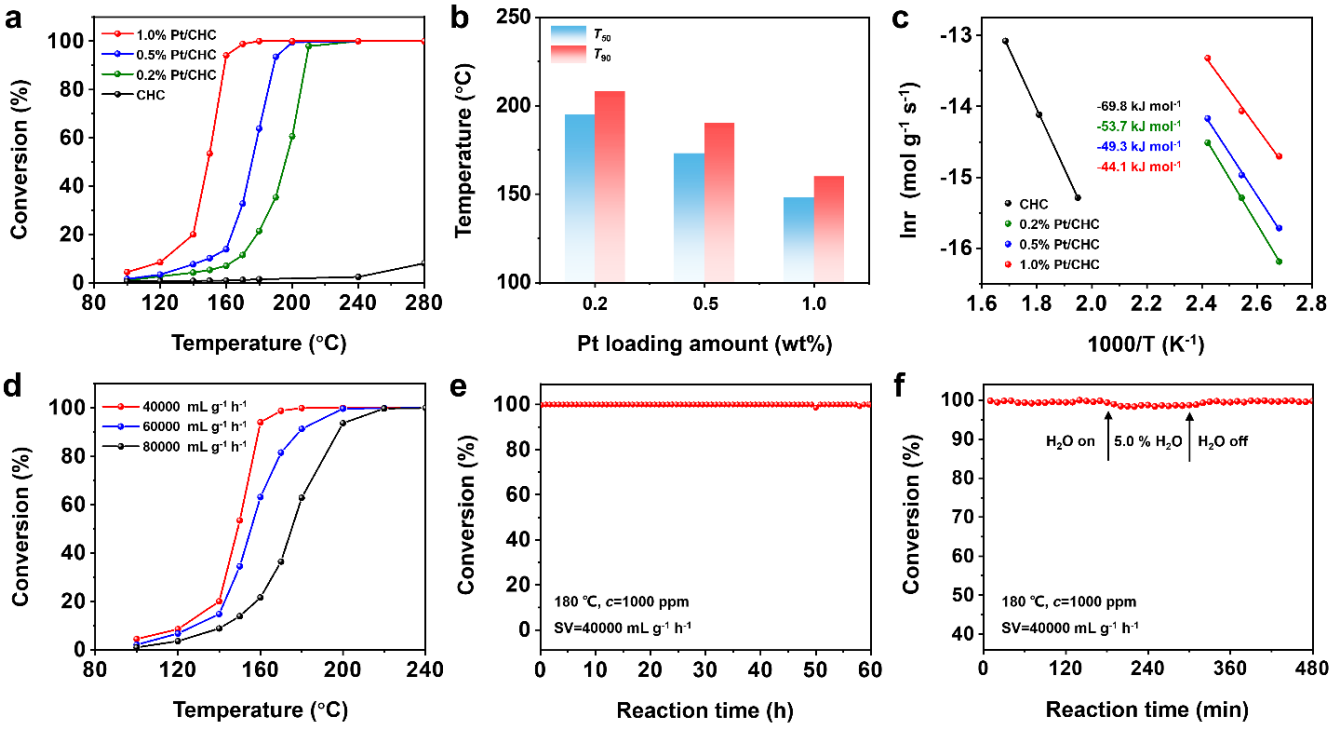

Fig. 6 Catalytic performance over Pt/CHC catalysts with different Pt loading amounts and CHC substrate. (a) Toluene conversion as a function of temperature of different samples. (b) Catalytic activity represented by T_{50} and T_{90} values over Pt/CHC catalysts. (c) Arrhenius plots for the oxidation of toluene over different catalysts. (d) Toluene conversion activity of 1.0% Pt/CHC catalyst at various flow rates. (e) Stability test of 1.0% Pt/CHC catalyst for toluene conversion. (f) Water effect on toluene conversion over 1.0% Pt/CHC catalyst.

(53.7 kJ mol^{-1}) Pt/CHC and CHC (69.8 kJ mol^{-1}), kinetically confirming the fact that the enhanced metal-support interaction due to Pt immobilization had significant influence on intrinsic activities of catalysts.[46] In addition, TOF_{Pt} and specific reaction rates were calculated at 140 °C to compare the catalytic activities of samples.[47,48] As displayed in Table S3, 1.0% Pt/CHC sample exhibited much higher TOF_{Pt} and specific reaction rates than those of comparative samples with different loading amounts, showing that the introduction of Pt nanoclusters of higher amounts had a greater enhancement on the catalytic activity. It is important to investigate the toluene oxidation over the catalysts at higher SV values for the practical application consideration. The effect of SV from 40000 to 80000 mL g^{-1} h^{-1} on toluene conversion over the 1.0% Pt/CHC catalyst were probed in Fig. 6d and the conversion dropped with a rise of SV at the same reaction temperature, as a result of the of the shortened contact between the reactants and the catalytic active sites.[49] Fig. S5 showed the effect of toluene concentration on the catalytic activity and the catalytic activity of 1.0% Pt/CHC decreased with the increasing concentration. The T_{90} was only about 20 °C higher when the concentration increased from 500 to 1500 ppm, further indicating the superior catalytic activity. The excellent stability of the as-synthesized 1.0% Pt/CHC was demonstrated in Fig. 6e through the long-term test at 180 °C and SV of 40000 mL g^{-1} h^{-1}. The catalyst maintained a high and stable conversion rate of nearly 100% for up to 60 h and almost no fluctuation could be observed during the reaction process. The morphology stability of the 1.0% Pt/CHC was demonstrated by a distribution histogram with an average size of 1.18 ± 0.11 nm based on the typical TEM image in Fig. S6, where almost no obvious agglomeration could be observed. In addition, water is known to exist as a typical factor causing activity decrease in catalytic combustion of VOCs, so it is necessary to investigate the water resistance property of catalysts.[50] As shown in Fig. 6f, when 5.0% water vapor was introduced into the reactor system at the temperature of 180 °C, only a small activity decline could be observed in the toluene conversion profile. The catalytic performance could be recovered in a short period of time after the removal of water vapor, proving the desirable resistance to water vapor in reaction atmosphere of the 1.0% Pt/CHC catalyst. A comparation with other catalysts on toluene oxidation performance over T_{50} and T_{90} values as well as reaction conditions were tabulated in Table S4, demonstrating that the 1.0% Pt/CHC displays competitive performance among recent reported results.

4. Conclusions

In summary, an efficient chemical wet ball-milling strategy was successfully developed to synthesis of Pt nanoclusters supported cordierite honeycomb ceramic catalysts with various Pt loading amounts with enhanced toluene oxidation performance. The as-synthesized 1.0% Pt/CHC catalyst achieved a 90% conversion rate toward 1000 ppm toluene at 160 °C under the SV of 40000 mL g^{-1} h^{-1}. The superior intrinsic kinetic of the 1.0% Pt/CHC sample was indicated by the E_a of 44.1 kJ mol^{-1}, much lower than those of other comparative samples. A distinguished long-term stability for more than 60 h and resistance properties to water vapor during reaction process were also experimentally demonstrated. The optimized performance can be ascribed to high adsorbed oxygen species, excellent low-temperature reducibility and enhanced metal-supported interaction between Pt nanoclusters and CHC substrate. Thus, the novel mechanochemical synthetic strategy paves a promising avenue to the large-scale production of supported noble metal catalysts with superior performance for practical environmental applications.

Acknowledgements

This study was supported financially by the Fundamental Research Funds for the Central Universities (2021XD-A04-1), the National Natural Science Foundation of China (Nos.61974011and51902027), the Fund of State Key Laboratory of Information Photonics and Optical Communications (Beijing University of Posts and Telecommunications, P. R. China).

Conflict of Interest

The authors declare no conflict of interest.

Supporting information

Applicable.

References

[1] W. C. Chung, D. H. Mei, X. Tu, M. B. Chang, *Catal. Rev.*, 2018, **61**, 270-331, doi: 10.1080/01614940.2018.1541814.

[2] H. Yuan, H. Peng, J. Guan, Y. Liu, J. Dai, R. Su, Z. Guo, Y. Chen, Q. Hu, B. Yuan, H. Wu, D. Kilula, I. Seok, *Eng. Sci.*, 2020, **9**, 68-76, doi: 10.30919/es8d910.

[3] Z. Sun, M. Wang, J. Fan, R. Feng, Y. Zhou, L. Zhang, *Adv. Compos. Hybrid Mater.*, 2021, **4**, 1322-1329, doi: 10.1007/s42114-021-00337-7.

[4] Z. Zhang, Z. Jiang, W. Shangguan, *Catal. Today*, 2016, **264**, 270-278, doi: 10.1016/j.cattod.2015.10.040.

[5] C. He, J. Cheng, X. Zhang, M. Douthwaite, S. Pattisson, Z. Hao, *Chem. Rev.*, 2019, **119**, 4471-4568, doi: 10.1021/acs.chemrev.8b00408.

[6] Z. Deng, Q. Zhang, Q. Deng, Z. Guo, I. Seok, *Adv. Compos. Hybrid Mater.*, 2021, 5, 491-503, doi: 10.1007/s42114-021-00345-7.

[7] M. N. Padvi, A. V. Moholkar, S. R. Prasad, N. R. Prasad, *Eng. Sci.*, 2021, **15**, 20-37, doi:10.30919/es8d431.

[8] Z. Bo, S. Yang, J. Kong, J. Zhu, Y. Wang, H. Yang, X. Li, J. Yan, K. Cen, X. Tu, *ACS Catal.*, 2020, **10**, 4420-4432, doi: 10.1021/acscatal.9b04844.

[9] C. Chen, J. Zhu, F. Chen, X. Meng, X. Zheng, X. Gao, F.-S. Xiao, *Appl. Catal. B-Environ.*, 2013, **199**, 140-141, doi: 10.1016/j.apcatb.2013.03.050.

[10] S. Ramalingam, A. Subramania, *Eng. Sci.*, 2021, **15**, 80-88, doi: 10.30919/es8d456.

[11] D. Xu, G. Huang, L. Guo, Y. Chen, C. Ding, C. Liu, *Adv. Compos. Hybrid Mater.*, 2021, 5, 113-129, doi: 10.1007/s42114-021-00317-x.
[12] Z. Bo, S. Yang, J. Kong, J. Zhu, Y. Wang, H. Yang, X. Li, J. Yan, K. Cen, X. Tu, *ACS Catal.*, 2020, **10**, 4420-4432, doi: 10.1021/acscatal.9b04844.
[13] R. Roy, D. Das, P. K. Rout, *Eng. Sci.*, 2021, **18**, 20-30, doi: 10.30919/es8d582.
[14] D. M. Gómez, J. M. Gatica, J. C. Hernández-Garrido, G. A. Cifredo, M. Montes, O. Sanz, J. M. Rebled, H. Vidal, *Appl. Catal. B-Environ.*, 2014, **144**, 425-434, doi: 10.1016/j.apcatb.2013.07.045.
[15] X. Chen, Z. Zhao, Y. Zhou, Q. Zhu, Z. Pan, H. Lu, *Appl. Catal. A-Gen.*, 2018, **566**, 190-199, doi: 10.1016/j.apcata.2018.08.025.
[16] W. Li, H. Ye, G. Liu, H. Ji, Y. Zhou, K. Han, *Chinese J. Catal.*, 2018, **39**, 946-954, doi: 10.1016/S1872-2067(18)63015-3.
[17] H. Zhao, H. Wang, Z. Qu, *J. Environ. Sci. (China)*, 2022, **112**, 231-243, doi: 10.1016/j.jes.2021.05.003.
[18] Y. Si, J. Li, B. Cui, D. Tang, L. Yang, V. Murugadoss, S. Maganti, M. Huang, Z. Guo, *Adv. Compos. Hybrid Mater.*, 2022, 1-16, doi: 10.1007/s42114-022-00446-x.
[19] L. Wu, J. Deng, Y. Liu, L. Jing, X. Yu, X. Zhang, R. Gao, W. Pei, X. Hao, A. Rastegarpanah, D. Hongxing, *J. Environ. Sci. (China)*, 2022, **116**, 209-219, doi: 10.1016/j.jes.2021.12.015.
[20] C. Chen, Q. Wu, F. Chen, L. Zhang, S. Pan, C. Bian, X. Zheng, X. Meng, F.-S. Xiao, *J. Mater. Chem. A*, 2015, **3**, 5556-5562, doi: 10.1039/c4ta06407k.
[21] S. Zhao, Y. Wen, X. Liu, X. Pen, F. Lü, F. Gao, X. Xie, C. Du, H. Yi, D. Kang, X. Tang, *Nano Res.*, 2020, **13**, 1544-1551, doi: 10.1007/s12274-020-2765-1.
[22] X. Liu, S. Jia, M. Yang, Y. Tang, Y. Wen, S. Chu, J. Wang, B. Shan, R. Chen, *Nat. Commun.*, 2020, **11**, 4240, doi: 10.1038/s41467-020-18076-6.
[23] T. Gan, J. Yang, D. Morris, X. Chu, P. Zhang, W. Zhang, Y. Zou, W. Yan, S. H. Wei, G. Liu, *Nat. Commun.*, 2021, **12**, 2741, doi: 10.1038/s41467-021-22946-y.
[24] K. Huang, L. Zhang, T. Xu, H. Wei, R. Zhang, X. Zhang, B. Ge, M. Lei, J. Y. Ma, L. M. Liu, H. Wu, *Nat. Commun.*, 2019, **10**, 606, doi: 10.1038/s41467-019-08484-8.
[25] S. Dey, G. C. Dhal, D. Mohan, R. Prasad, *Adv. Compos. Hybrid Mater.*, 2020, **3**, 84-97, doi: 10.1007/s42114-020-00139-3.
[26] K. Huang, R. Wang, S. Zhao, P. Du, H. Wang, H. Wei, Y. Long, B. Deng, M. Lei, B. Ge, H. Gou, R. Zhang, H. Wu, *Energy Storage Mater.*, 2020, **29**, 156-162, doi: 10.1016/j.ensm.2020.03.026.
[27] P. P. Bag, *Eng. Sci.*, 2021, **13**, 98-105, doi: 10.30919/es8d1004.
[28] Z. Sun, X. Huang, A. Xia, Z. Yan, L. Qian, *Eng. Sci.*, 2021, **16**, 19-25, doi: 10.30919/es8d564.
[29] K. Kubota, Y. Pang, A. Miura, H. Ito, *Science*, 2019, **366**, 1500-1504, doi: 10.1126/science.aay8224.
[30] F. Zhang, W. Cheng, Z. Yu, S. Ge, Q. Shao, D. Pan, B. Liu, X. Wang, Z. Guo, *Adv. Compos. Hybrid Mater.*, 2021, **4**, 1330-1342, doi: 10.1007/s42114-021-00346-6.
[31] K. Huang, Z. Zhao, H. Du, P. Du, H. Wang, R. Wang, S. Lin, H. Wei, Y. Long, M. Lei, W. Guo, H. Wu, *ACS Sustain. Chem. Eng.*, 2020, **8**, 6905-6913, doi: 10.1021/acssuschemeng.0c00830.
[32] K. Huang, S. Guo, R. Wang, S. Lin, N. Hussain, H. Wei, B. Deng, Y. Long, M. Lei, H. Tang, H. Wu, *Chinese J. Catal.* 2020, **41**, 1754-1760, 10.1016/S1872-2067(20)63613-0.
[33] P. Du, K. Huang, X. Fan, J. Ma, N. Hussain, R. Wang, B. Deng, B. Ge, H. Tang, R. Zhang, M. Lei, H. Wu, *Nano Res.*, 2021, **15**, 3065-3072, doi: 10.1007/s12274-021-3963-1.
[34] F. Li, G. F. Han, H. J. Noh, I. Ahmad, I. Y. Jeon, J. B. Baek, *Adv. Mater.*, 2018, **30**, e1803676, doi: 10.1002/adma.201803676.
[35] X. Fan, P. Du, X. Ma, R. Wang, J. Ma, Y. Wang, D. Fan, Y. Long, B. Deng, K. Huang, H. Wu, *Materials*, 2021, **14**, 2426, doi: 10.3390/ma14092426.
[36] I. J. Shon, H. S. Kang, J. M. Doh, J. K. Yoon, *Mat. Sci. Eng. A*, 2014, **606**, 139-143, doi: 10.1016/j.msea.2014.03.095.
[37] X. Li, J. Yan, K. Zhu, *Eng. Sci.*, 2021, **15**, 38-46, doi: 10.30919/es8d432.
[38] K. Huang, R. Wang, H. Wu, H. Wang, X. He, H. Wei, S. Wang, R. Zhang, M. Lei, W. Guo, B. Ge, H. Wu, *J. Mater. Chem. A*, 2019, **7**, 25779, doi: 10.1039/C9TA07469D.
[39] T. Gan, X. Chu, H. Qi, W. Zhang, Y. Zou, W. Yan, G. Liu, *Appl. Catal. B-Environ.*, 2019, **257**, 117943, doi: 10.1016/j.apcatb.2019.117943.
[40] J. Kong, Z. Xiang, G. Li, T. An, *Appl. Catal. B-Environ.*, 2020, **269**, 118755, 10.1016/j.apcatb.2020.118755.
[41] R. Peng, X. Sun, S. Li, L. Chen, M. Fu, J. Wu, D. Ye, *Chem. Eng. J.*, 2016, **306**, 1234-1246, doi: 10.1016/j.cej.2016.08.056.
[42] Z. Abbasi, M. Haghighi, E. Fatehifar, S. Saedy, *J. Hazard. Mater.*, 2011, **186**, 1445-1454, 10.1016/j.jhazmat.2010.12.034.
[43] B. Wang, B. Chen, Y. Sun, H. Xiao, X. Xu, M. Fu, J. Wu, L. Chen, D. Ye, *Appl. Catal. B-Environ.*, 2018, **238**, 328-338, doi: 10.1016/j.apcatb.2018.07.044.
[44] Z. Wang, H. Yang, R. Liu, S. Xie, Y. Liu, H. Dai, H. Huang, J. Deng, *J. Hazard. Mater.*, 2020, **392**, 122258, doi: 10.1016/j.jhazmat.2020.122258.
[45] Z. Wang, P. Ma, K. Zheng, C. Wang, Y. Liu, H. Dai, C. Wang, H. C. Hsi, J. Deng, *Appl. Catal. B-Environ.*, 2020, **274**, 118963, doi: 10.1016/j.apcatb.2020.118963.
[46] Y. He, F. Guo, K. R. Yang, J. A. Heinlein, S. M. Bamonte, J. J. Fee, S. Hu, S. L. Suib, G. L. Haller, V. S. Batista, L. D. Pfefferle, *J. Am. Chem. Soc.*, 2020, **142**, 17119−17130, doi: 10.1021/jacs.0c07179.
[47] M. Zhang, S. Zou, S. Mo, J. Zhong, D. Chen, Q. Ren, M. Fu, P. Chen, D. Ye, *Chemosphere*, 2021, **262**, 127738, doi: 10.1016/j.chemosphere.2020.127738.
[48] G. Liu, Y. Tian, B. Zhang, L. Wang, X. Zhang, *J. Hazard. Mater.*, 2019, **367**, 568-576, doi: 10.1016/j.jhazmat.2019.01.014.
[49] S. Xie, H. Dai, J. Deng, H. Yang, W. Han, H. Arandiyan, G. Guo, *J. Hazard. Mater.*, 2014, **279**, 392-401, doi: 10.1016/j.jhazmat.2014.07.033.
[50] S. Kang, M. Wang, N. Zhu, C. Wang, H. Deng, H. He, *Chinese Chem. Lett.*, 2019, **30**, 1450-1454, doi: 10.1016/j.cclet.2019.03.023.

Author Information

Peng Du *received his B.E. degree from Harbin Institute of Technology in 2018. He is now pursuing his Ph.D. degree at School of Science, Beijing University of Posts and Telecommunications. His current research interests are focused on the heterogeneous catalysts for energy and environmental applications.*

Ming Lei *received his M.D. at State Key Laboratory of Materials Composites and Advanced Technology, Wuhan University of Technology in 2004. Then, he received his Ph.D. from the Laboratory of Nanophysics and Devices, Institute of Physics, Chinese Academy of Sciences in 2007. He worked as a postdoctoral fellow at The Hong Kong University of Science and Technology (2007-2008) and the Chinese University of Hong Kong (2009-2010). He is now a professor and doctoral supervisor of the School of Science, Beijing University of Posts and Telecommunications. He has long been engaged in the preparation of low dimensional nano materials, photoelectric properties and device applications.*